MAINTAINING HIGH SUPPORT STIFFNESS

Spherical flexure joints with three degrees of freedom are typically limited to small deflections, because when deflected they lose a great deal of stiffness in support directions. To allow for a larger range of motion while maintaining high support stiffness, an advanced stacked folded-leafspring-based spherical joint has been developed. Optimisations of this design have led to a spherical joint with a 30° range of tilt motion in combination with a high support stiffness (> 200 N/mm) and load capacity (> 290 N).

MARK NAVES, RONALD AARTS AND DANNIS BROUWER

Introduction

In high-precision applications, flexure-based mechanisms are used for their deterministic behaviour because of the absence of play and friction. Spherical flexure joints are often encountered in spatial precision manipulators with parallel kinematic arrangements and sub-micron repeatability, such as spatial (6-DoF) nanopositioners, and micro-assembly and precision alignment systems (DoF = degree of freedom). For this purpose, spherical notch joints or short-wire flexures are typically used to provide the required spherical motion. These joints can be realised in a small, compact design that allows for easy manufacturing (Figure 1a).

They only provide, however, a limited range of motion (typically a few degrees) due to their localised compliance, which results in high stress levels at even small deflection angles. Therefore, they are mostly used for optical alignment systems that require only small rotation angles of the spherical joints. Larger ranges of motion can be obtained by a stacked arrangement of wire flexures (Figure 1b) or by concatenating three single-DoF flexure joints in series in order to obtain the required DoFs (Figure 1c). However, these types of joints typically suffer from a limited support stiffness, as well as a large decrease of this support stiffness with increasing deflection angle due to the large deformations involved.

To allow for a larger range of motion in combination with high support stiffness, a flexure-based spherical joint design is presented here that uses folded leafsprings as flexible elements to obtain the required DoFs. A folded-leafspring-based design for a spherical joint has been presented before by Schellekens et al. [1], who combined three parallel folded leafsprings. This design allowed for a high support stiffness and load capacity, although only a limited range of motion was obtained.

In order to extend the range of motion while maintaining high support stiffness, an advanced stacked folded-leafspring-based spherical joint has been developed for use in a fully-flexure-based hexapod system with a large range of motion. A schematic overview of this system is illustrated in Figure 2 and a CAD rendering is provided in Figure 3.

AUTHORS' NOTE

Mark Naves (Ph.D. student) and Dannis Brouwer (professor) are members of the chair of Precision Engineering, and Ronald Aarts (associate professor) is a member of the chair of Structural Dynamics, Acoustics & Control, all in the Department of Mechanics of Solids, Surfaces & Systems at the University of Twente, Enschede (NL).

m.naves@utwente.nl
www.utwente.nl/en/et/ms3

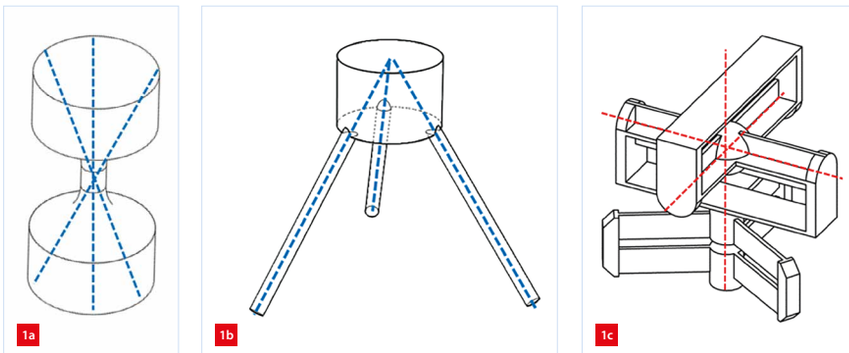

Flexure-based spherical joints.
(a) Spherical notch joint or short-wire flexure.
(b) Wire-flexure-based spherical joint.
(c) Spherical joint constructed by concatenating three single-DoF joints.

Folded-leafspring-based spherical joint

A spherical flexure joint is characterised by the property of allowing motion in the three rotational DoFs, while

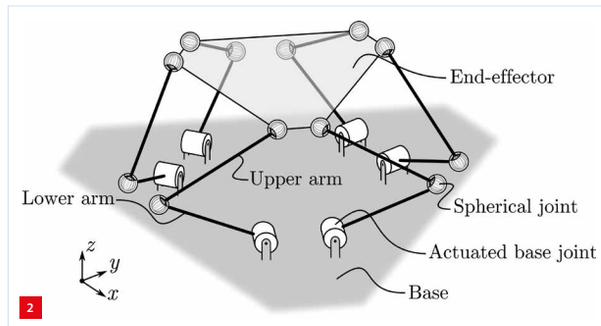

Schematic of the kinematics of the hexapod system (T-flex).

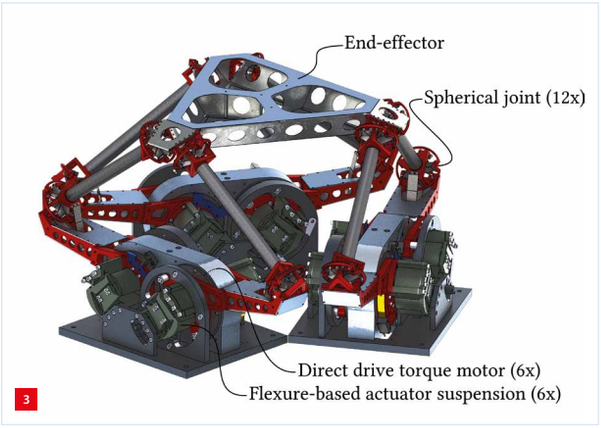

Rendering of the fully-flexure-based hexapod system (T-flex).

constraining motion in all translational directions (the directions in which load-bearing support is provided). For many applications, a spherical joint with coinciding rotation axes is required to concentrate all rotational motion in a single point.

In order to obtain the three rotational DoFs for the spherical joint, flexible elements were required that provide the necessary constraints. Wire flexures are suited to this purpose, but they do not allow for both a large range of motion and a high support stiffness [2]; see, e.g., the wire-flexure-based design as presented in Figure 1b. Therefore, folded leafsprings were used, which also constrain a single translational DoF that is located along the fold line, equivalent to the wire flexure. Compared to wire flexures, the folded leafsprings typically allow for a larger range of motion with a higher level of support stiffness and load capacity.

The most elementary topology for a folded-leafspring-based spherical flexure joint consists of a set of folded leafsprings directly connecting the fixed world and the end-effector. An exactly constrained design was obtained with three folded leafsprings as illustrated in Figure 4.

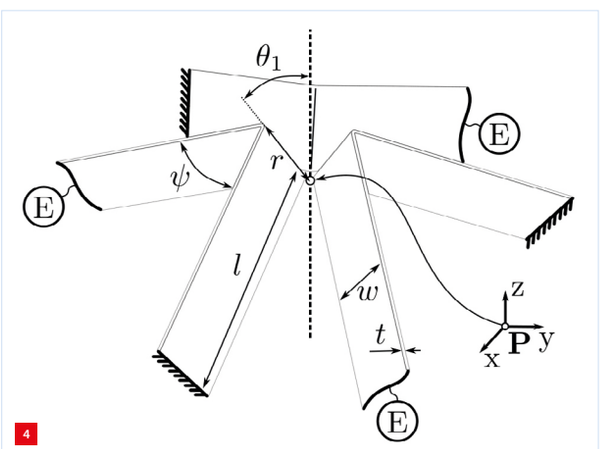

Parameterised folded-leafspring-based spherical-joint topology with 'E' representing the connection with the end-effector.

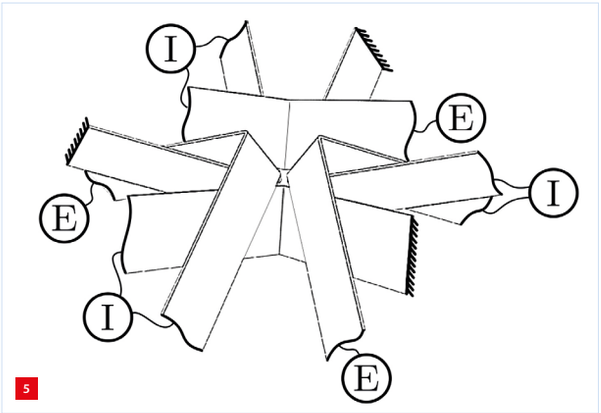

Serially stacked folded-leafspring-based spherical-joint topology with 'E' representing the connection with the end-effector and 'I' representing the connection to an intermediate stage.

To increase the range of motion of this folded-leafspring-based spherical-joint topology, a serially stacked equivalent topology was suggested. This topology consists of two sets of three leafsprings, with the first three leafsprings connecting the fixed world and an intermediate body, and the second set connecting the intermediate body and the end-effector. Effectively, this leads to two spherical joints stacked in series with coinciding rotation axes, each contributing to half of the motion.

Additionally, by properly stacking the folded leafsprings, they can be placed close together (and intertwined), leading to a compact design. As the deflection per stage is halved, the stress levels in the flexures are reduced, allowing for thicker leafsprings, which results in increased support stiffness. Furthermore, because the support stiffness decreases progressively nonlinearly with the deflection, halving the deflection leads to (far) less than half the stiffness loss over the range of motion. A schematic overview of the serially stacked folded-leafspring-based joint topology, referred to as the SFL-joint, is provided in Figure 5.

It has to be noted that the intermediate body is only constrained for translational motion and therefore contains three redundant rotational DoFs (the intermediate body is three times underconstrained). For most flexure mechanisms, underconstrained intermediate bodies dramatically impair support stiffness (particularly when the mechanism is in a deflected state) due to the coupling of external loads and the underconstrained DoFs, such as the compounded parallel leafspring guidance without slaving [3].

For the SFL-joint, however, the instant centres of rotation of the intermediate body and the end-effector coincide, and barely change position for an increasing deflection angle. Hence, external loads on the end-effector do not result in reaction moments in the DoFs of the intermediate

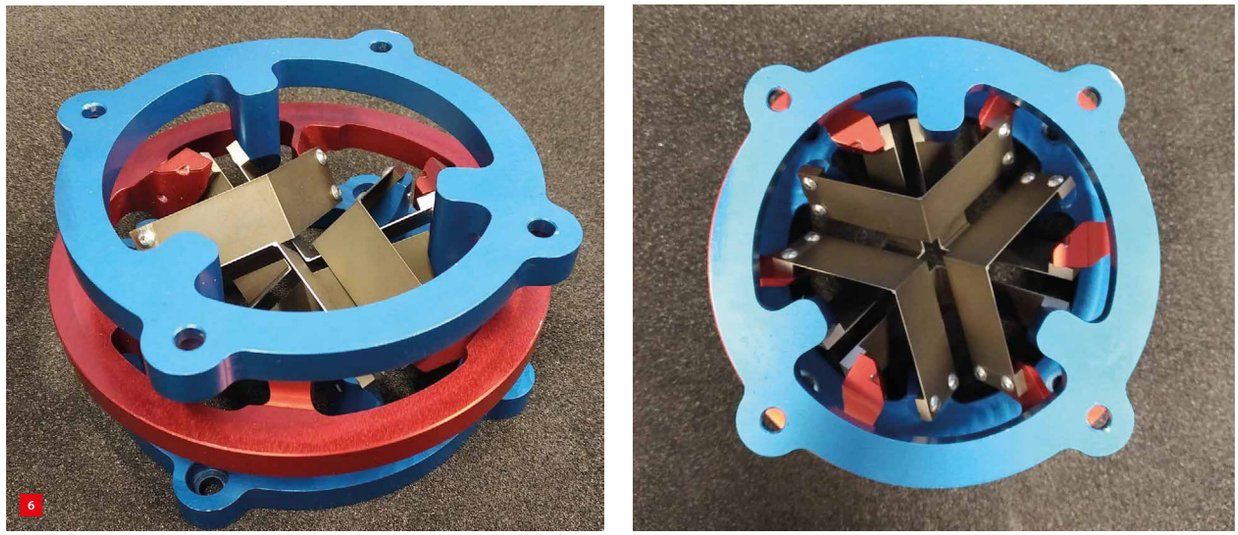

Two views of a realisation of the SFL-flexure joint. Diameter of the red intermediate body is 140 mm and the height of the joint is 70 mm.

body. Additionally, as the rotation centres coincide, rotational motion of the intermediate body does not contribute to translational motion of the end-effector. Due to this special property, support stiffness does not deteriorate due to the underconstrained intermediate body and the position of the end-effector is not influenced by the motion of the intermediate body.

However, with respect to the dynamic behaviour of the joint, having an underconstrained intermediate body can result in unwanted vibrations in the system due to its low eigenfrequency. These vibrations can be reduced by adding damping to the intermediate body (e.g. eddy-current damping) to reduce the magnitude of the vibrations [4].

Optimisation of the joint geometry

Due to the complex spatial geometry of the spherical flexure joint as presented in Figure 5, deriving a 'good' geometry that results in a high-performing design is a far from trivial task, especially when considering the possibility of collision of the flexures given the large range motion. Predicting mechanism designs that are free of collision can be hard, given the 3D nature of the motion in combination with the large deformations.

Therefore, the design of the flexure joint was optimised by a shape-optimisation algorithm that searches for the optimal geometry for the flexure joint. The algorithm maximises support stiffness, taking into account the workspace and collision of the flexures. For this optimisation, the flexible multi-body software SPACAR [5] was used to evaluate the deformations, support stiffness and maximum stress in the flexures for a given geometry in combination with a specifically developed collision-detection algorithm [6]. For the optimisation, we considered a range of motion of 30° tip-tilt (ω_t: rotation around the x/y-axis) and 10° pan

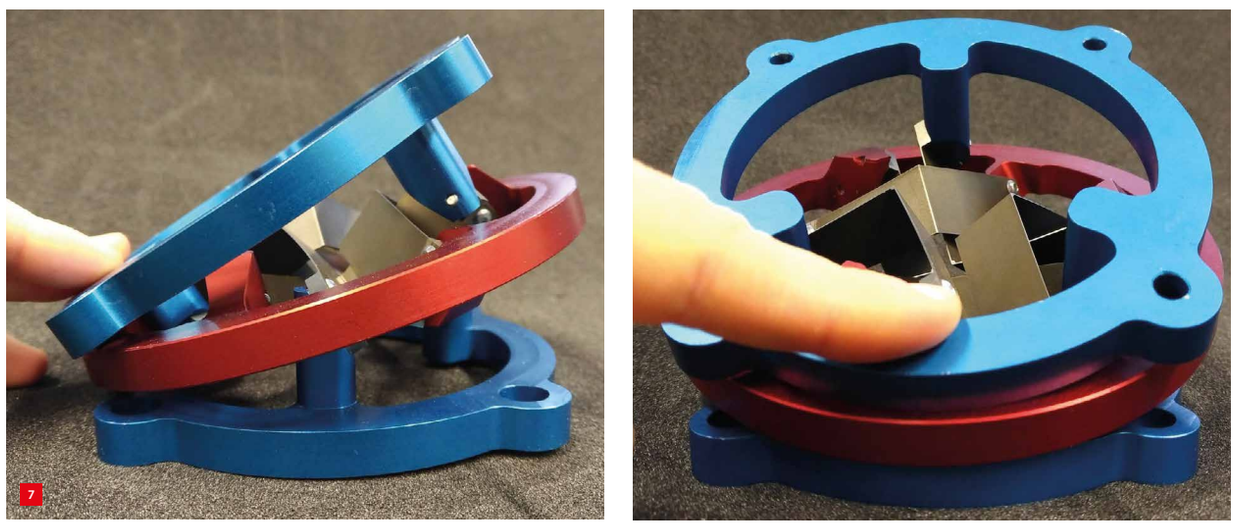

Two views of the SFL-flexure joint in a deflected state.

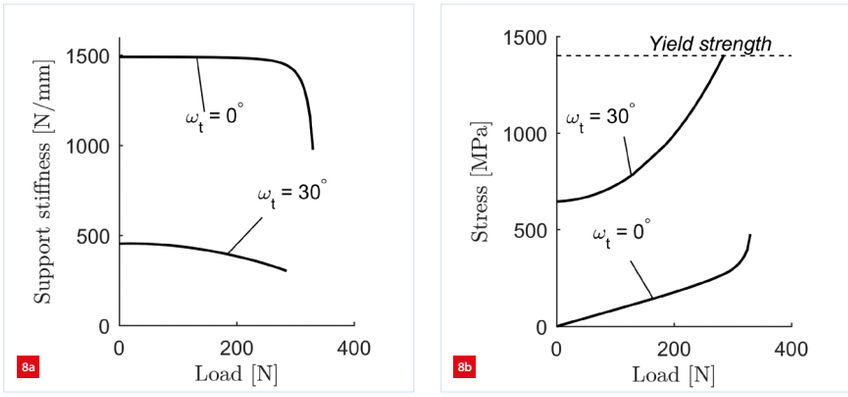

Flexure behaviour as a function of load applied along the pan axis.
(a) Support stiffness along the pan axis.
(b) Simulated (von Mises) stress.

(ω_p: rotation around the *z*-axis). Tool steel (yield strength: 1,400 MPa) was the material of choice, amply allowing the imposed stress limit of 600 MPa. Based on the optimisation results, a prototype of this spherical joint has been constructed. A realisation of the prototype in undeflected and deflected states is provided in Figures 6 and 7. This prototype was constructed from tool steel flexures of 0.4 mm thickness combined with three aluminium frame bodies (the base and end-effector anodised in blue, the intermediate body anodised in red).
The resulting optimal design showed a support stiffness of the flexures in the main load-carrying direction (along the vertical *z*-axis) of about 1,500 N/mm when not deflected and a stiffness of almost 500 N/mm at a maximum tilt angle of 30°. Furthermore, the joint allows for a maximum load (in the same direction) of approximately 300 N. The support stiffness and maximum stress in the flexures for increasing load (for both 0° and 30° tilt angle) are provided in Figure 8. Note that at 0° tilt, load capacity is limited by the buckling of the flexures, resulting in an instanteneous, strong decrease in support stiffness at a load of approximately 290 N. However, at a tilt angle of 30°, load capacity is limited by the maximum stress in the flexures, exceeding the yield strength at about 300 N.

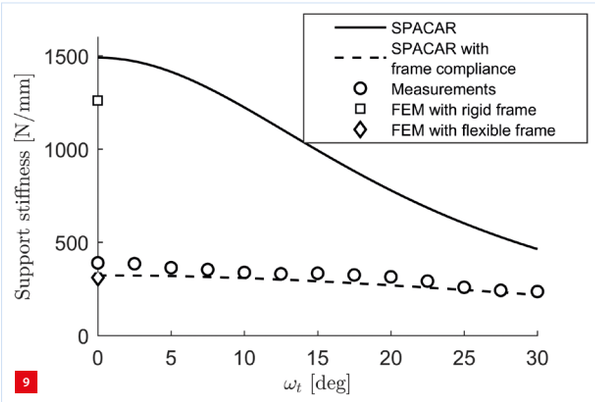

Experimental validation including flexible multi-body simulations (SPACAR), FEM simulations (SolidWorks Simulation) and measurements.

Experimental validation

To validate the support stiffness, an experimental validation was conducted. To that end, the joint was deflected up to the desired tilt angle and kept at this angle by means of a fixture. Furthermore, load was applied to the joint by a micrometer connected to the joint via a single wire flexure (attached to a force sensor to measure the applied load). Deflection of the joint was measured by a capacitive displacement sensor. As both the applied force and deflection were measured, this allowed for the evaluation of the support stiffness of the joint.

An overview of the measured and simulated stiffnesses as functions of the tilt angle (ω_t) is provided in Figure 9. Especially with small tilt angles, the measured stiffness (circles) is substantially lower than simulated (solid line). This difference in support stiffness can be related to additional compliance introduced by the frame parts that connect the leafsprings, and the way folded leafsprings typically load connecting parts by moments. During the design of the spherical joint, care was taken to ensure high stiffness of the frame parts.
Despite this, restrictions on the design freedom imposed by avoiding any collision of the flexures and frame parts over the range of motion inherently limit the stiffness of the frame. Therefore, the additional compliance of the frame has to be taken into account to accurately assess the support stiffness of the entire joint.

To evaluate the effect of frame compliance on the overall support stiffness, a finite-element method (FEM) analysis (Solidworks Simulation) considering zero tilt-angle was conducted, both for a flexible and a rigid frame. The overall stiffness of the joint appeared to be $1.3{\cdot}10^3$ N/mm considering rigid frame parts. Stiffness decreased to $3.1{\cdot}10^2$ N/mm for a realistic representation of the frame. From these values, an approximation of the frame stiffness could be computed, assuming the flexures and frame stiffness are in series, resulting in an equivalent frame stiffness of $4.1{\cdot}10^3$ N/mm.

By adding this equivalent frame stiffness in series to the stiffness obtained from numerical simulations, an approximate stiffness could be estimated (dashed line). When frame compliance was added to the simulations, a good match was obtained between experiment and simulations. Additionally, the maximum load capacity of the joint was verified, which showed a load capacity of at least 150 N. Higher loads have not been validated in order to prevent plastic deformations of the flexures that would compromise other measurements.

Spherical joint redesign

Based on the results and the experimental validation, a redesign of the spherical joint with 25° tip-tilt and 10° pan

Realisation of the redesign of the SFL-flexure joint. Frame parts are given in orange, diameter 90 mm. Note that the connections with the intermediate body are concentrated at three locations, in contrast to the six locations in the design presented in Figure 6, thus reducing frame compliance.
(a) Full spherical joint.
(b) Spherical joint with top and bottom frame parts detached.

motion was proposed, offering a higher level of support stiffness (500 N/mm at maximum tilt angle including frame compliance), as illustrated in Figure 10. This increased support stiffness was primarily obtained by changing the stacking order of the flexures in order to connect the folded leafsprings more closely together on the intermediate body, thus reducing frame compliance. Furthermore, the size of the joint has been reduced to a diameter of 90 mm and a height of 60 mm, allowing for an additional reduction in compliance of the frame parts and a reduction of its footprint.

Conclusion

A large-range-of-motion spherical flexure joint can be obtained by using a topology with three or more folded leafsprings in parallel, of which all folding lines intersect at a single point. Range of motion can be greatly increased by effectively stacking two spherical joints in series, each having three folded leafsprings in parallel. With this design, the deformations of the flexures are halved, allowing for stiffer flexures at the same level of stress. This results in a significant increase in support stiffness, although it comes at the cost of an underconstrained intermediate body with a potentially low eigenfrequency.

Structural optimisations on this flexure joint have resulted in a flexure-based spherical joint that allows for 30° tip-tilt and 10° pan motion. At maximum deflection, this joint maintains a support stiffness of over 200 N/mm, which is more than an order of magnitude higher than the current state-of-the-art spherical flexure joints with similar range of motion. Furthermore, a load capacity of almost 300 N at maximum tilt angle has been obtained. Experimental validations verified the simulated performance and confirmed the high support stiffness and load capacity over the entire range of motion.

REFERENCES

[1] Schellekens, P., Rosielle, N., Vermeulen, H., and Vermeulen, M., "Design for precision: current status and trends", *CIRP Annals – Manufacturing Technology*, 47, pp. 557-586, 1998.
[2] Soemers, H., *Design principles for precision mechanisms*, T-Pointprint, Enschede, 2010.
[3] Jones, R.V., "Some uses of elasticity in instrument design", *Journal of Scientific Instruments*, 39(5), pp. 193-203, 1962.
[4] Naves, M., Aarts, R.G.K.M., and Brouwer, D.M., "Large stroke high off-axis stiffness three degree of freedom spherical flexure joint", *Precision Engineering*, 56, pp. 422-431, 2019.
[5] Jonker, J.B., and Meijaard, J.P., "SPACAR – computer program for dynamic analysis of flexible spatial mechanisms and manipulators", pp. 123-143, in Schiehlen, W. (ed.), *Multibody Systems Handbook*, Springer-Verlag, Heidelberg, 1990.
[6] Naves, M., Aarts, R.G.K.M., and Brouwer, D.M., "Efficient collision detection method for flexure mechanisms comprising deflected leafsprings", *Journal of Mechanisms and Robotics*, 10(6), 7 pages, 2018.

Wim van der Hoek's design principles

The design principle 'control of degrees of freedom' underlies the kinematic concept described here. A (remote) centre of rotation has been created by having three wire flexures point at one location. The equivalent kinematic structure can then be created by exchanging each wire-flexure for a folded leafspring to increase off-axis stiffness and load capacity.